Journal of Engineering Research and Reports

Volume 26, Issue 12, Page 316-327, 2024; Article no.JERR.128510
ISSN: 2582-2926

Study of the Parameters of Anchor Body in-Water Motion in the Array Anchor Technique

Wang Zheng [a*]

[a] *School of Mechanical Engineering, North China University of Water Resources and Electric Power, Zhengzhou, China.*

Author's contribution

The sole author designed, analysed, interpreted and prepared the manuscript.

Article Information

DOI: https://doi.org/10.9734/jerr/2024/v26i121360

Open Peer Review History:
This journal follows the Advanced Open Peer Review policy. Identity of the Reviewers, Editor(s) and additional Reviewers, peer review comments, different versions of the manuscript, comments of the editors, etc are available here: https://www.sdiarticle5.com/review-history/128510

Original Research Article

Received: 15/10/2024
Accepted: 17/12/2024
Published: 26/12/2024

ABSTRACT

When the rocket anchor enters the water, the projectile body hits the water surface and is subject to a great impact force, which may cause the failure of the internal zero devices and the damage of the anchor structure in serious cases, leading to the failure of the breach sealing mission. Therefore, it is particularly important to study the load characteristics of the anchor body in the process of water entry. In this paper, a numerical simulation of the anchor body in the process of water entry is carried out, focusing on the load distribution of the projectile body and other situations, which can provide certain guidance and reference for the structural design of the rocket anchor.

In this paper, based on the LS-DYNA module in Workbench, the flow-solid coupling numerical simulation of the anchor body water entry process is carried out by using the ALE method, and the motion law and load distribution of the anchor body under different water entry speeds, different water entry angles and different sizes are investigated and the pressure distribution of the flow field is analyzed, and the equivalent stresses of the upper, middle and lower parts of the rocket anchors

**Corresponding author: Email: 1477875115@qq.com;*

Cite as: *Zheng, Wang. 2024. "Study of the Parameters of Anchor Body in-Water Motion in the Array Anchor Technique". Journal of Engineering Research and Reports 26 (12):316-27. https://doi.org/10.9734/jerr/2024/v26i121360.*

under different working conditions are compared and analyzed. analyzed. The results show that the maximum impact force of the anchor body at water entry is linearly related to the water entry velocity, and reducing the water entry angle can effectively reduce the maximum impact force on the rocket anchor itself; for the rocket anchor structures with different sizes, the change of the force in the lower part is positively correlated to the size of the structure; the change of the stress in the middle part is not obvious; and the equivalent force in the upper part is in a fluctuating state, and with the increase of the structure of the rocket anchor, the smaller the fluctuating peak value is.

Keywords: Anchor body in water; ALE; fluid-consolidation coupling; stress changes.

1. INTRODUCTION

China is a flood-prone country with frequent breaches. Floods during the flood season cause dam breaches seriously threaten local agriculture, transportation, ecological environment and the lives and property of nearby residents. River dam failure is related to the national economy and people's livelihood, and it is urgent to plug the breach (Chen, 2020). At present, the method used to plug the river, generally to the breach free throw plugging materials, mostly throw willow pillow stone, geotechnical package, large concrete and other materials (Chen et al., 2022); because of its stability coefficient in the breach at the underwater only 0.7 ~ 0.8 and lead to plugging the long time required, and even the vast majority of plugging materials because of the poor stability of the high-speed current is often washed away and rushed downstream resulting in plugging low material utilization, usually, the actual use of plugging materials on site is 1.5 times of the theoretical calculation, and even up to 2 times more if encountering rapids, so the cost of plugging materials is huge (Cheng et al., 2022). Currently relying on the wreck of the wreck to plug the restoration of the emergency response method is obviously in urgent need of improvement and enhancement (Fan et al., 2022). The difficulty of sealing the breach is: after the breach occurs, the location of the mouth door is often larger than the drop, coupled with a larger flood discharge, resulting in a higher flow rate, the plugging material is difficult to stabilize in the riverbed; and the larger plugging material is subjected to some of the limitations of the construction machinery and equipment (Gui, 2020). Therefore, it is necessary to design and develop a more advanced and scientific solidification technology and casting method for the plugging material (Hou, 2021). For the current situation of shipwrecks and wrecks plugging, the development of a fast, safe and efficient new technology for breach rescue (Huang & Le, 2016). The use of rocket boost directed launch rocket anchor with anchor cable, relying on the rocket anchor very high operating speed to get rid of the impact of the high speed water flow at the mouth of the ulcer, the anchor body into the depth of the soil layer, the rocket anchor with the tail with the anchor cable and the shore fixed piles for connection, for the follow-up steel mesh gabions and other materials to provide a stable stronghold for plugging the mouth of the material through the multi-point shot anchor, from point to point into a slice, weaving into the anchor array, for the follow-up pushed into the gabion network to provide landing point, to ensure that gabions play a blocking role in the breach (Chen et al. 2022, Wu et al. 2015, Liu et al. 2024).

2. THEORY OF LS-DYNA BASED INCOMING WATER CALCULATION

The important feature of fluid-solid coupled mechanics is the interaction between two-phase media, the deformation of the solid in the fluid under the action of deformation or movement, the deformation or movement of the solid in turn affects the distribution of the field of the fluid. The coupled equation can be defined by the coupled solid-fluid coupling problem, the coupled equation is characterized by the definition of the domain of the existence of both solid domain and fluid domain, the unknown variables are both solid variables and fluid variables (Li, 2020). The reason why the solid and fluid domains cannot be solved separately is due to this feature of the coupled equations (Liu et al., 2024). Assuming that the fluid is an ideal fluid (non-viscous, non-swirling, incompressible) and the structure is a linear elastic material, the basic equations are established (Sui, 2023).

2.1 Fluid Domain Equations

(1) Continuum equation:

$$\rho_0 v_{i,j} = -\dot{\rho}(i = 1,2,3)$$

$$\rho_0\left(\frac{\partial v_x}{\partial x} + \frac{\partial v_y}{\partial y} + \frac{\partial v_z}{\partial z}\right) = -\frac{\partial \rho}{\partial t}$$

Where, $\dot{\rho}$ —Change in mass density due to perturbation;

ρ_0 —The mass density of the fluid before the perturbation.

(2) Equations of motion:

$$\rho_0 \dot{v}_i = -p_i (i = 1,2,3)$$

Where, p_i —Disturbance-induced pressure changes in the flow field;

$\dot{v}_i$ —Flow velocity component of a fluid disturbance.

(3) Equation of state:

$$\rho = \frac{\rho_0}{\kappa} p$$

Where, ϰ—Bulk modulus of a fluid.

(4) Flow field equation:

Combining the above three equations and eliminating $\dot{v}_i$and ρ from the equation yields the following flow field equation:

$$p_{ii} - \frac{1}{c^2} \ddot{p} \vDash 0$$

Where, $c = \sqrt{k/\rho_0}$—Speed of sound in a flow field.

(5) Fluid boundary condition:

Rigid solid boundary: $\frac{\partial p}{\partial n_f} = 0$

free level:$\frac{\partial p}{\partial z} + \frac{1}{g} \ddot{p} = 0$

2.2 Solid Domain Equation

Ontological relationship:

$$\sigma_{ij} = \mu(u_{i,j} + u_{j,i}) + \lambda u_{k,k} \delta ij$$

Where, μ and λ is the Lame's constant, which is converted to the modulus of elasticityE and Poisson's ratio σ as follows:

$$\lambda = \frac{\sigma E}{(1+\sigma)(1-2\sigma)}$$

$$\mu = \frac{E}{2(1+\sigma)}$$

Solid boundary conditions:

Force boundary condition：$\sigma_{ij} n_{sj} = \bar{T}_i$

Displacement boundary conditions：$u_i = \bar{u}_i$

Where, u_i—Known displacement components on the solid;

$\bar{u}_i$—Known surface force components on a solid.

2.3 Flow-solid Interface Equations

In the flow-solid interface to meet the following conditions and establish the relevant equations:

(1) The normal velocity at the fluid-solid interface is continuous.

$$v_{fn} = v_f \cdot n_f = v_s \cdot n_f = -v_s \cdot n_s = v_{sn}$$

Combined with the fluid equations of motion

$$\frac{\partial p}{\partial n_i} + \rho_f \ddot{u} n_f = 0$$

Where, $\ddot{u}$—Solid displacement vector;

ρ_f—Fluid mass density.

(2) Continuous normal force at the flow-solid interface

$$\sigma_{ij} n_{sj} = \tau_{ij} n_{fj} = -\tau_{ij} n_{sj}$$

Where, τ_{ij} —Components of the fluid stress tensor.

2.4 For non-Viscous Fluids

$$\tau_{ij} = -p\delta_{ij}$$

$$\sigma_{ij} n_{sj} = p n_{si}$$

Lagrange, Euler, and ALE algorithms

Lagrange, Euler, and ALE algorithms are three commonly used algorithms in LS-DYNA.

(1) Lagrange Algorithm
The Lagrangian algorithm is widely used *to solve the stress-strain of solid* structures. In this algorithm, the material

is attached to the mesh, and the material will be deformed with the movement of the mesh, so it can accurately capture the movement of the structural boundary, but for dealing with large deformation problems due to the distortion of the mesh, it will produce large numerical errors (Wang, 2023).

(2) Euler's algorithm

Euler (Euler) algorithm in which the grid is fixed in spatial coordinates and the material moves in the grid. This algorithm can effectively solve the fluid flow and solid large deformation problems, but can not accurately describe the movement of the structural boundary (Wang et al., 2021).

(3) Arbitrary Lagrange-Euler method

The Arbitrary Lagrangian-Eulerian (ALE) algorithm is similar to the Eulerian algorithm, but the spatial mesh in the ALE algorithm can be moved freely to accurately capture the motion of the solid boundary, so it has the advantages of both Lagrangian and Eulerian algorithms, and it is widely used in solving the coupled fluid-solid problems. When the ALE algorithm is used, one or several Lagrange time steps are performed first, at which time the cell mesh is deformed with the flow of the material, and then the ALE time steps are performed: (1) keep the boundary conditions of the deformed structure, re-divide the internal mesh, and keep the mesh topology unchanged (Wu et al., 2015); (2) transport the variables such as the density and energy of structural cells in the deformed mesh, as well as the velocity of the nodes, to the re-divided mesh, and the velocity vector is transferred to the re-divided grid. vectors are transported to the new mesh after re-demarcation (Zhang, 2019). The variables of each cell solution are transported during the solution, and the number of variables depends on the material model; for the cells containing the equation of state, only the density, internal energy, and shock wave viscosity are transported (Zheng, 2020). At present, the ALE cell algorithms in the LS-DYNA program mainly include single-point ALE, single-point multi-matter ALE, and single-point single-matter with cavity integration algorithms; the transport algorithms mainly include Donor Cell algorithm with first-order accuracy and Van Leer algorithm with second-order accuracy.

Among the three algorithms, the Lagrangian algorithm is more accurate and efficient, but it is not suitable for dealing with large deformation; the ALE and Euler algorithms are suitable for solving large deformation problems, but the computational efficiency and accuracy are lower. In this paper, the single-point multi-material ALE algorithm is selected for the air and water units, and the Van Leer+HIS (Half-Index-Shift) algorithm with second-order accuracy is selected for the transport algorithm.

3. SIMULATION AND ANALYSIS OF ANCHOR BODY ENTERING WATER

This chapter mainly studies the load characteristics of the anchor body in the early stage of water entry-impact stage and open vacuole stage, based on the LS-Dyna module in the finite element software Workbench, numerical calculations of fluid-solid coupling of the anchor body of the shell structure into the water, and it is proposed to get the relevant parameters affecting the maximum impact load of the anchor body into the water, which is an important reference for the subsequent structural design of the rocket anchor. The model is of important reference for the design of subsequent rocket anchors.

3.1 Three-Dimensional Modeling

In the simulation of rocket anchor entering water, the model consists of three parts: air domain, fluid domain - water domain and rocket anchor. In the process of calculation, the dimensions of air domain and fluid domain are 1500mm×1000mm×1000mm, the diameter of the anchor body is φ60mm, the diameter of the back end is φ100mm, and the overall length is 1000mm. the simulation model is shown in the figure below:Methanol is a colorless, transparent, highly volatile, flammable and water-soluble liquid. Methanol has the molecular formula CH3OH and contains 50% of its own oxygen, which facilitates complete combustion of the fuel. The boiling point is 64.7℃, which is lower than gasoline and easy to mix with air; the ignition limit of methanol is 7.3%~36.9%, which is easier to ignite than gasoline; the octane number of methanol is 110, which is higher than gasoline and has good anti-explosion property, which is conducive to improving the compression ratio of the engine and enhancing the efficiency;

methanol is easily soluble in water, easily degradable and does not cause any damage to the soil. Methanol is easily soluble in water, easily degradable, and does not pollute soil and rivers; methanol is liquid at room temperature, so it is convenient to transport, store and refill.

In order to facilitate the establishment of the underwater motion model of the projectile, the following reasonable assumptions need to be made on the projectile

1) Neglect the gravity effect during the projectile entering the water;
2) The projectile does not rotate after entering the water;
3) The resistance of the projectile is opposite to the direction of the velocity, and its direction coincides with the tangent of the ballistic path.

3.2 Analysis of Calculation Results

1) Analysis of fluid domain calculation results

Shell structure anchor body in the water at the moment of entry into the water and the anchor head contact part of the water body will produce a huge pressure peak, and then this pressure peak to the surrounding water body propagation; with the continuous absorption of the water medium, the pressure is gradually reduced. As the anchor advances, the water in contact with the head of the anchor generates a pressure peak, which decreases as the speed of the anchor decreases.

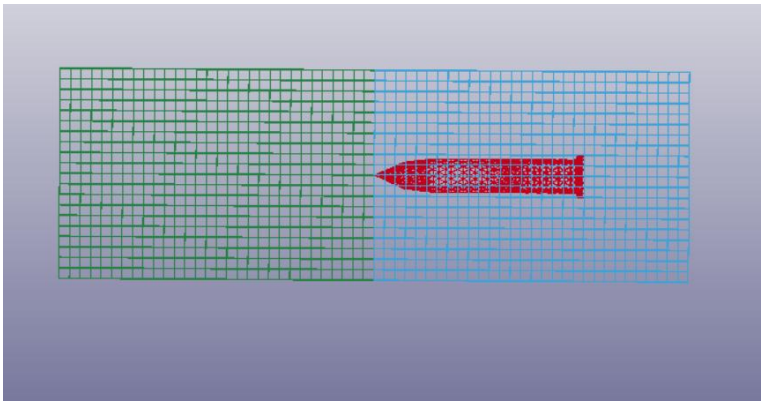

Fig. 1. Anchor entry simulation model

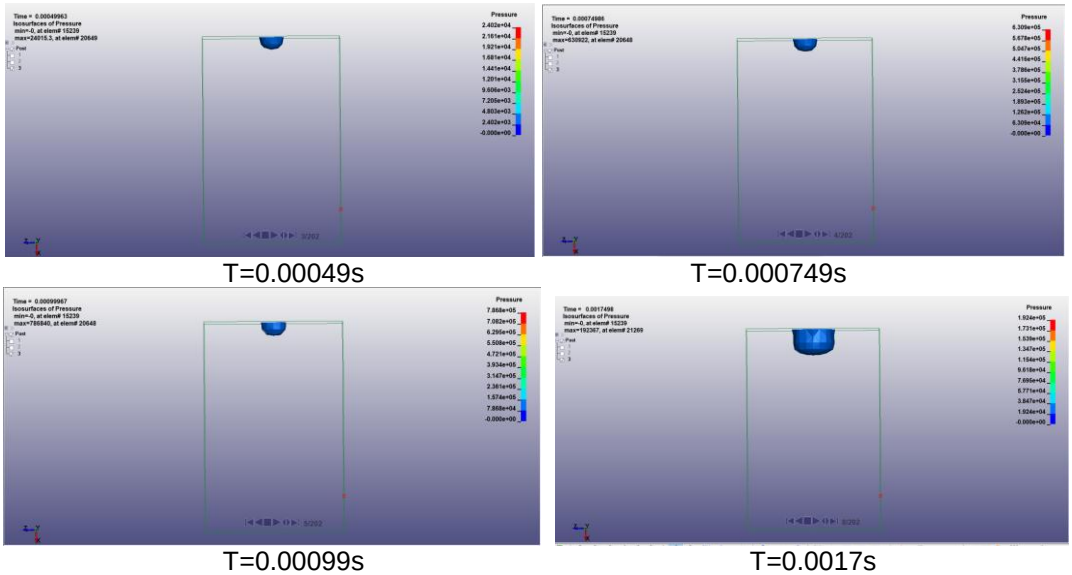

Fig. 2. Partial momentary pressure contour maps of the fluid domain

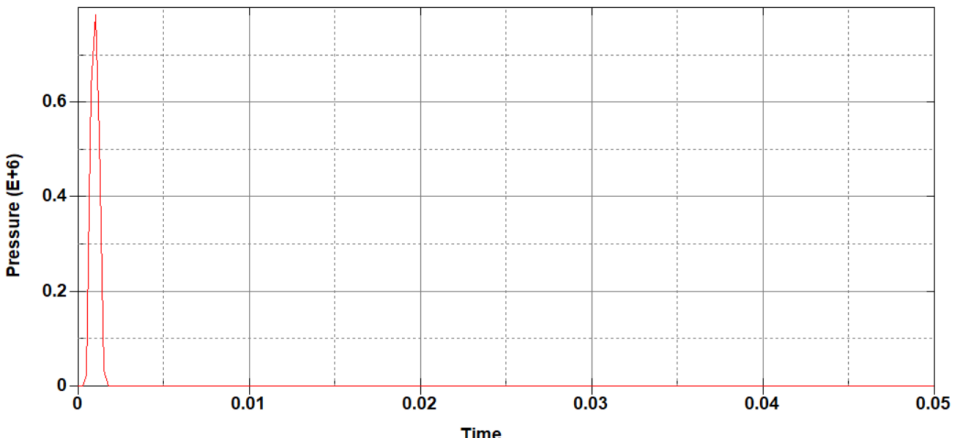

Fig. 3. Pressure time course curve of the unit with the maximum pressure peak in the fluid domain

Fig. 3 is the anchor body and the fluid domain contact point where the unit, when the anchor body impact on the water surface, the pressure rises rapidly to reach a peak of 0.775MPa, after the pressure here to the surrounding propagation of the sudden decrease, so the first peak after the gradual decrease to maintain stability.

2) Rocket anchor structure analysis

Fig. 4 shows the variation curve of the motion parameters of the anchor body with time. Since the anchor body is a rotary body, only the displacement, velocity and acceleration in the X direction are analyzed. The motion trend is shown in the following figure, the displacement of the shell structure anchor body in the X direction is basically a straight line with equal slope. When the anchor body slams the water surface, the water surface will give the anchor body a huge reaction force, resulting in a peak acceleration of about 949M/S², at this time, the anchor body velocity decay faster, between 0s and 0.1s have a large acceleration, 0.01s after the velocity drops to about 23m/s; in 0.01s after the acceleration value of the fluctuation of a regular but the peak value in the gradual decrease in the velocity After 0.01s, the acceleration value fluctuates regularly but the peak value decreases gradually, and the velocity decreases gradually, and the velocity decay graph is also similar to a straight line with equal slope.

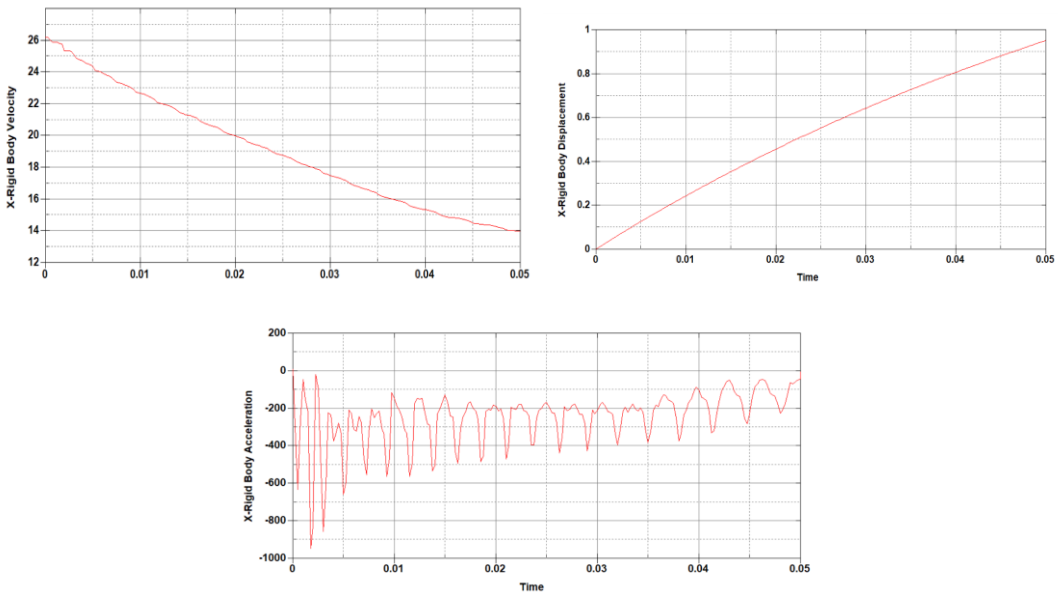

Fig. 4. Variation curves of kinematic parameters during the rocket anchor entry process

Fig. 5 shows the equivalent cloud diagram of the anchor body at some moments. The anchor body model is in direct contact with the fluid domain at the beginning, so at the moment of water entry, the tip of the head hits the water surface to produce a huge stress concentration phenomenon, and at the same time is subjected to the reverse force of the water body and is transmitted to the X reverse direction, which produces a large stress peak at the upper end, i.e., the tail part of the anchor body, and produces an equivalent stress of up to 821.5Mpa at T=0.00049S, which is more than the material's yield stress, the duration is not long, but the material will deform, in the subsequent T = 0.0017s, T = 0.007s, T = 0.01225s, the anchor body corresponding to the stress of 329Mpa, 195Mpa, 162.3Mpa, respectively, the anchor body after the stage of hitting the water, due to the inertia continues to advance into the water, at this time the acceleration change is small, the stress generated in the head will also be Decrease, because for a certain moment, in addition to the early stage of water impact, there may be more than one stress concentration inside the anchor body, one is in the head due to the anchor body continues to push the water body and the rest is the location of the previous stress wave propagation process to the tail, the tail of the anchor body will continue to have stress concentration phenomenon, compared to the moment of entry into the water, the peak value is gradually reduced, accompanied by the phenomenon of oscillation.

3) Variation of forces at different locations of the anchor body

Comprehensive comparison of Figs. 6, 7, 8, the bottom and middle part of the unit appears earlier in the stress peak time, but the value of the stress peak is smaller than the tip, because the tip of the beginning of the direct contact with the fluid domain, so the bottom of the stress peak appeared earlier for 0.00025s before and after, the middle unit of the stress peak appeared and the bottom of the unit appeared at a time close to the time, behind 0.00005s, almost the same time to reach peak value The stress peak value of the top unit is larger than that of the bottom and middle units, because the reaction force generated by the tip needs to be transferred, so the stress peak value of the top unit occurs later, about 0.0005s before and after the stress peak value is due to the anchor body into the water caused by the moment of water collision, the value of about 424Mpa, which is not more than the yield stress limit of the material. As mentioned in the previous section, in addition to the initial stage of water impact, there may be multiple stress concentrations inside the anchor body, one at the head due to the constant advancement of the anchor body into the body of water, and the rest at the location where the previous stress wave propagated to the top, the top of the anchor body will also continue to produce a stress concentration, compared to the instant of water ingress, the peak gradually decreases, accompanied by oscillations, which is consistent with the stress change in the figure.

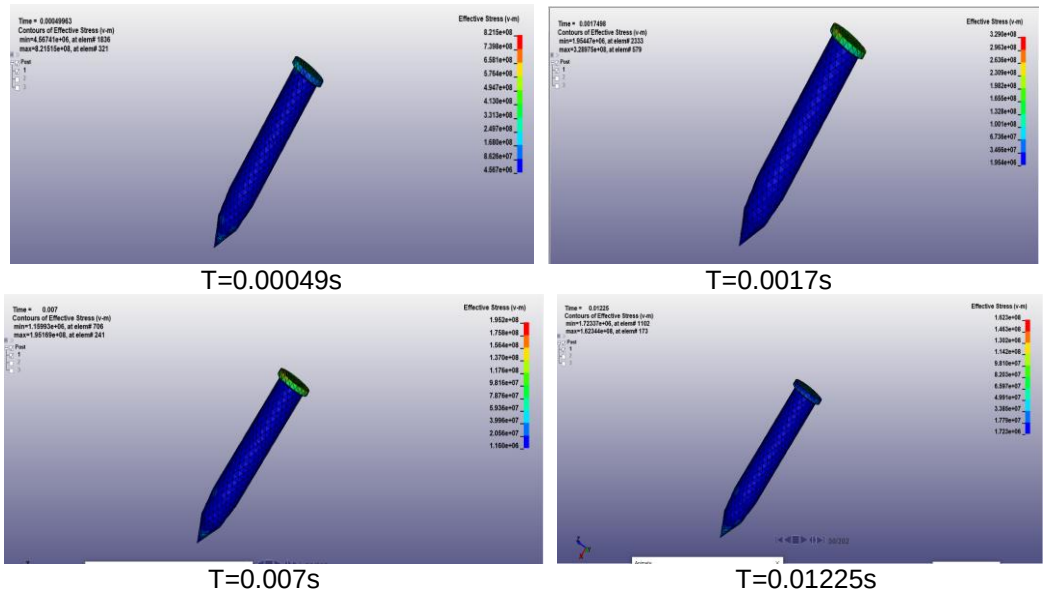

Fig. 5. Equivalent cloud diagram for some moments of the anchor body

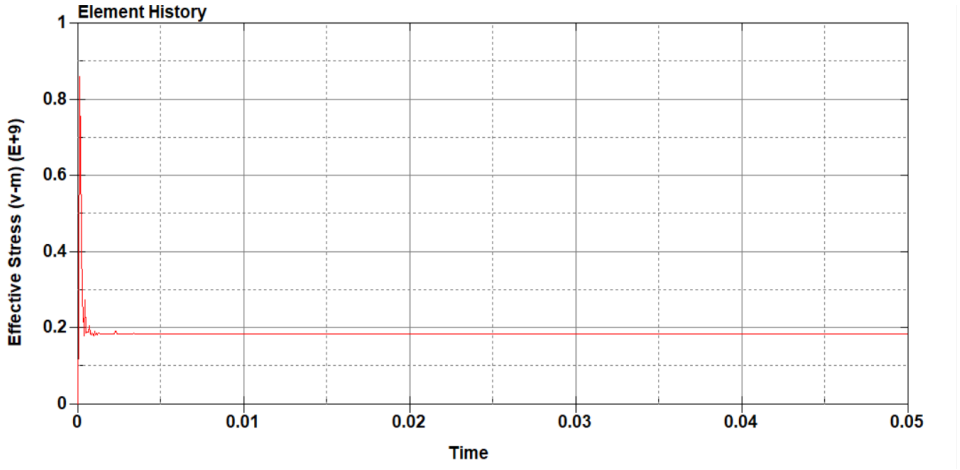

Fig. 6. Equivalent cloud diagram of the tip unit of the anchor body

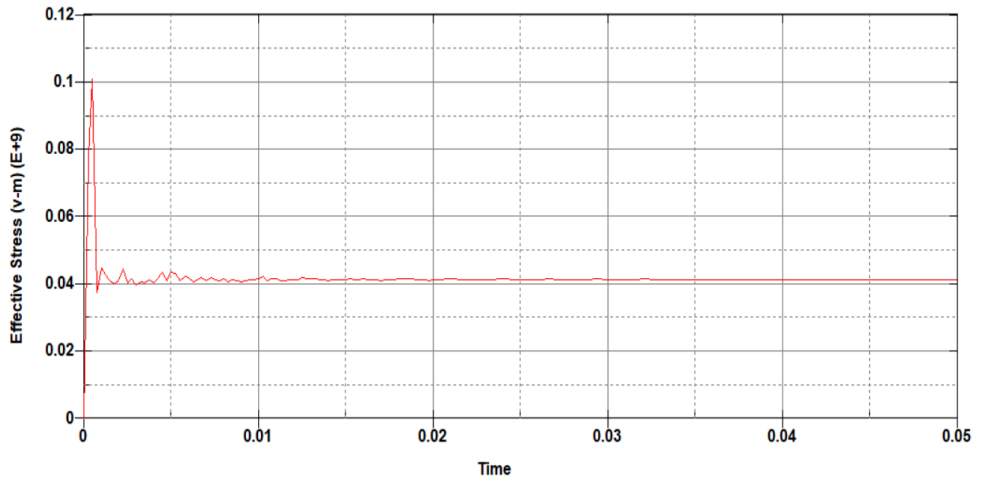

Fig. 7. Equivalent cloud diagram of the middle unit of the anchor body

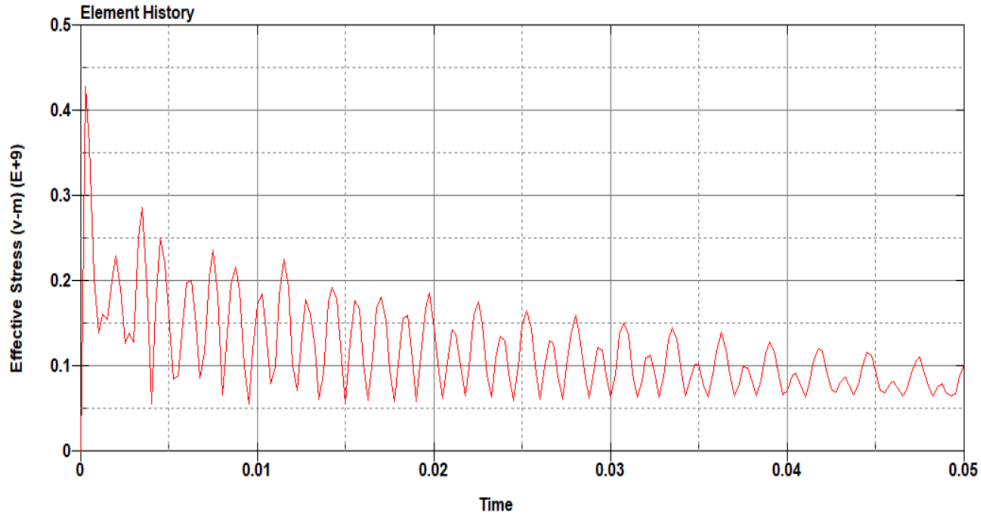

Fig. 8. Equivalent cloud diagram of the upper end unit of the anchor body

4) Influence of velocity on the impact load of the projectile body into the water

The maximum pressure of the unit in the fluid domain is monitored, and Fig. 9 shows the pressure time course curves of the same unit in the fluid domain in contact with the anchor body under three different working conditions. The anchor body is in direct contact with the fluid domain at the beginning, so the time of the pressure peak of the fluid domain unit under the three working conditions is almost the same, which is the instant of contact, and then gradually reduced to 0. When the initial speed of the anchor body is 30m/s, the maximum pressure of the fluid domain unit is 0.4Mpa; when the initial speed is 50m/s, the maximum pressure is 0.78Mpa; when the initial speed is 60m/s, the maximum pressure is 0.9Mpa. By comparing the specific values, when the structure of the anchor body is certain, the maximum impact pressure on the fluid domain is proportional to the initial velocity of the anchor body, the greater the initial velocity, the greater the impact pressure of the anchor body on the fluid; the smaller the initial velocity, the smaller the impact pressure of the anchor body on the fluid.

The anchor body is subjected to external forces when it enters the water, which is reflected in the stress changes inside the anchor body. When the anchor sails in the air domain, the stress inside the anchor body is zero; when it hits the water, the anchor body is subjected to an impact force in an instant, and a huge stress distribution occurs in the head and propagates to the tip. Comparison of the three working conditions of the anchor body internal units subjected to the maximum equivalent stress, as shown in Fig. 10, because the anchor body in the water when the impact force with the acceleration linearly related to the acceleration, and the change of acceleration and the change of the anchor body's speed has a direct link, the anchor body from the air medium into the water medium, due to the huge difference in density, regardless of the size of the initial speed, in the instant of the impact of the water speed has a tendency to infinitely converge to zero. Therefore, the greater the initial velocity, the greater the acceleration generated by the impact, the greater the impact force, the greater the stress inside the anchor body. Therefore, at the initial stage of the anchor body into the water, the stress of the internal unit is the largest when the initial velocity is 50m/s, and the smallest when it is 30m/s. After the anchor body passes through the water impact stage, it continues to advance into the water due to inertia, at which time the change in acceleration is smaller and the stress generated

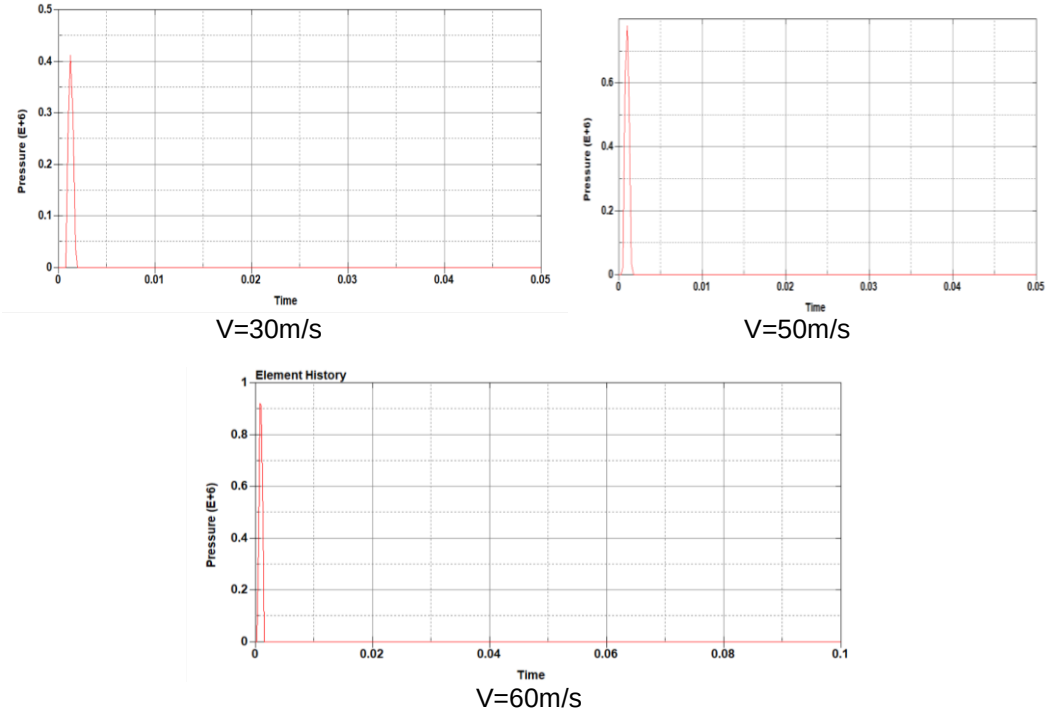

Fig. 9. Maximum equivalent force of the internal unit of the elastic body at each moment of the three working conditions

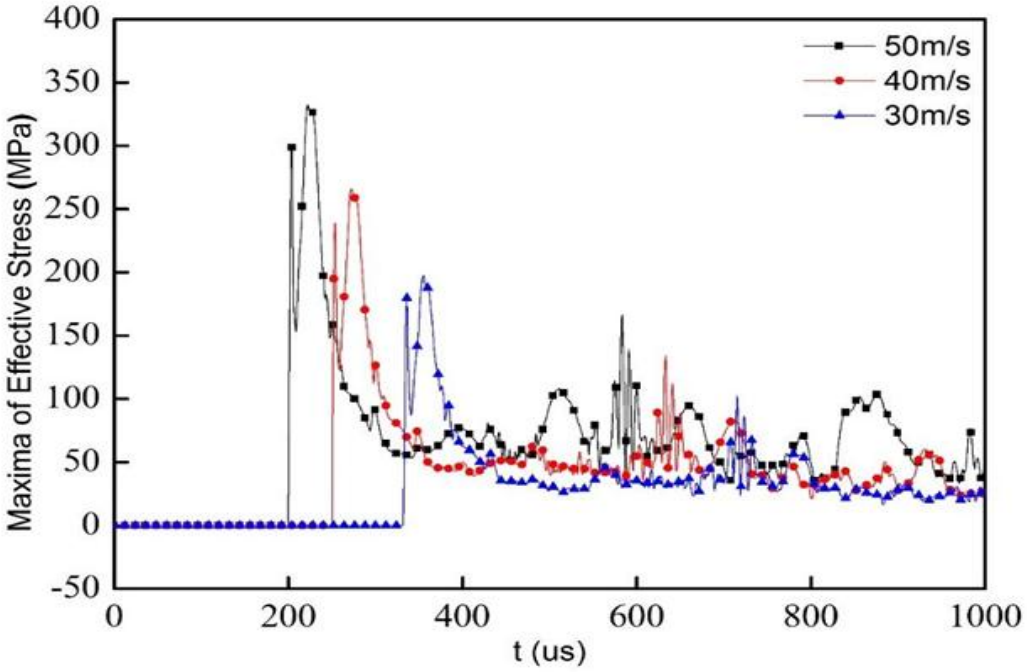

Fig. 10. Maximum equivalent force of the internal unit of the elastic body at each moment under the three working conditions

in the head decreases, because for a certain moment, except for the initial stage of water impact, there may be multiple stress concentrations inside the anchor body, one at the head due to the continuous advancement of the elastic body into the water, and the rest at the location where the previous stress wave is located during its propagation to the tail. When the anchor body enters the water in the unpowered section, its internal stresses gradually decrease and level off as the anchor body continues to advance, but are still accompanied by oscillations due to the transmission of the stress wave.

Through the calculation of different initial velocity anchor body into the water found that the greater the speed, the greater the peak impact pressure generated by the waters, the maximum equivalent force inside the anchor body will also increase, and the maximum equivalent force and speed is basically a linear relationship; anchor body in the process of entering the water, every 250us or so, will periodically produce a large stress peak, but are less than the stage of the impact of the water, and therefore focus on considering the elasticity of the body during this period of time. Therefore, we focus on the stress situation of the elastic body during this time to ensure the safety of the elastic body structure.

4. CONCLUSION

It can be seen from the analysis of the above results:

(1) In the simulation process of anchor body entering water, the pressure of the fluid domain by the anchor body just contact reached the peak, with the anchor body gradually into the water pressure gradually becomes smaller, and the peak pressure appears in the tip of the anchor body and the fluid domain in contact with the unit at the distance from the anchor body into the water at the unit, the more the distance, the smaller the pressure, and the peak pressure occurs at a time lagging behind the contact unit.

(2) Anchor body into the water process, speed change, displacement change is basically a straight line with equal slope, due to the moment of impact will produce a great reverse force, so the acceleration in the moment of entry into the water to reach a peak, with the anchor body into the water, there will be more than one stress concentration phenomenon, so the acceleration presents an oscillatory state, but the peak is much smaller than the moment of entry into the water.

(3) Anchor body into the water in the process of the upper, middle and lower three parts will produce different sizes of force, but the stress of the largest part of the emergence of the top, with the passage of time in each part of the peak equivalent force were downward trend, so in the design process of the anchor structure, should be referenced to the instantaneous top of the force into the water, to ensure that the rocket anchor structure to complete the normal blocking task.

(4) The same structure of the rocket anchor, with different initial speed into the water when the pressure generated by the fluid domain is different, the greater the initial speed, the greater the pressure on the fluid domain; through the calculation of different initial speed of the anchor body into the water found that the greater the speed, the greater the impact pressure generated by the waters of the peak value of the anchor body, the maximum equivalent force inside the anchor body will also increase, and the maximum equivalent force and the speed of the basic is a linear relationship, followed by the presentation of the oscillating The maximum equivalent force is basically linearly related to the velocity, and then shows oscillation, but the peak value is smaller than the moment of water impact.

DISCLAIMER (ARTIFICIAL INTELLIGENCE)

Author(s) hereby declare that NO generative AI technologies such as Large Language Models (ChatGPT, COPILOT, etc) and text-to-image generators have been used during writing or editing of this manuscript.

COMPETING INTERESTS

Author has declared that no competing interests exist.

REFERENCES

Chen, W. (2020). Simulation of the stability and vacuole characteristics of a projectile across medium at high speed into water stage (Doctoral dissertation). Harbin Engineering University. DOI:10.27060/d.cnki.ghbcu.2020.002304.

Chen, X., Liu, B., & Le, G. (2022). Numerical simulation research on the anchor last deployment of marine submersible buoy system based on VOF method. *Journal of Marine Science and Engineering, 10*(11), 1681.

Cheng, W., Wang, H., Xiong, G., et al. (2022). Shock response simulation of projectile water entry process based on LS-DYNA. *Military Automation, 41*(01), 86-89.

Fan, X. D., Chia, C. C., Wang, X., et al. (2022). Research on the impact characteristics of high-speed projectile into water based on ALE method. *Journal of Jiangsu University of Science and Technology (Natural Science Edition), 36*(02), 7-14.

Gui, S. (2020). Fluid-solid coupling analysis of the impact process of a high-speed projectile into water (Doctoral dissertation). Nanjing University of Aeronautics and Astronautics. DOI:10.27239/d.cnki.gnhhu.2020.000018.

Hou, Y. (2021). Research on the kinetic characteristics of hollow projectile entering water at low speed (Doctoral dissertation). Nanjing University of Science and Technology. https://doi.org/10.27241/d.cnki.gnjgu.2021.002350.

Huang, K., & Le, S. W. (2016). Experimental study on the phenomenon of water entry of different head type projectile models. *Physical Experiment, 36*(05), 13-18.

Li, G. (2020). Numerical study on the fluid-solid coupling characteristics of a projectile entering water at low speed (Doctoral dissertation). Harbin Engineering University. DOI:10.27060/d.cnki.ghbcu.2020.001582.

Liu, G., Jia, P., Sun, J., Jiang, Z., Yang, F., Yang, G., & Shao, G. (2024). Research and application of new anti-floating anchor in anti-floating reinforcement of existing underground structures. *Frontiers in Earth Science, 12*, 1364752.

Sui, Y. (2023). Characterization of fluid-solid coupled loads for the projectile body-in-water problem with different head shapes (Doctoral dissertation). Harbin Engineering University. DOI:10.27060/d.cnki.ghbcu.2023.000648.

Wang, L. (2023). Research on cavitation fluid characteristics of high-speed projectile across medium into water (Doctoral dissertation). Southwest University of Science and Technology. DOI:10.27415/d.cnki.gxngc.2023.000997.

Wang, Z., Wu, M. L., & Sun, Y. S. (2021). Analysis of factors and parameters

affecting the flow-solid coupling of multi-media ALE method. *Computer Simulation, 38*(02), 18-23.

Wu, X., Gunnu, G. R. S., & Moan, T. (2015). Positioning capability of anchor handling vessels in deep water during anchor deployment. *Journal of Marine Science and Technology, 20*, 487-504.

Zhang, Z. (2019). Research on the initial characteristics of rotary body entering water at high speed (Doctoral dissertation). Harbin Engineering University.

Zheng, L. (2020). Research on the water entry process of projectile across medium (Doctoral dissertation). Harbin Engineering University. DOI:10.27060/d.cnki.ghbcu.2020.000558.

Peer-review history:
The peer review history for this paper can be accessed here:
https://www.sdiarticle5.com/review-history/128510